KFUPM
Journal of Undergraduate Research International

Diamond Open Access

Development of a Microwave Metamaterial Sensor for Noninvasive Glucose Detection

Dhay Al-Harthi and Ibraheem Al-Naib*

Cite https://doi.org/10.64589/juri/221324

Submitted: November 27, 2025 **Revised:** March 22, 2026 **Accepted:** March 25, 2026

ABSTRACT

Diabetes is a chronic disease requiring frequent monitoring. However, traditional methods are invasive and can cause discomfort. Although prior studies have focused on various microwave and metamaterial geometries in noninvasive sensor applications, they exhibit multiple limitations, including the need for large sample volumes and complex fabrication processes. In this study, a noninvasive microwave sensor was designed, fabricated, and evaluated for fingertip glucose detection. The proposed sensor comprises a single-metal-layer coplanar waveguide with four nested split-ring resonators on an FR4 substrate to enhance electric field confinement and maximize the interaction with biological samples. Experimental validation was performed using a Vector Network Analyzer with various concentrations of glucose samples ranging from 100 to 400 mg/dL. The sensor exhibited a general structural resonance near 4.18 GHz, whereas distilled water measurements exhibited a resonance at 3.584 GHz, which shifted with increasing glucose concentration, yielding a sensitivity of approximately 36.4 kHz/(mg · dL^{-1}). These findings highlight the potential of the compact microwave metamaterial sensor as a foundation for real-time glucose-monitoring systems.

Keywords: microwave biosensor, glucose monitoring, split-ring resonator, noninvasive sensing

1. INTRODUCTION

Diabetes is a chronic disease that occurs when the body either cannot produce insulin or use it effectively. Over time, this limitation causes severe damage to the heart, kidneys, eyes, and other vital organs. According to the World Health Organization, diabetes affects approximately 830 million people worldwide, with the majority living in low- and middle-income countries [1]. Traditional glucose measurement methods, such as finger-prick blood glucose tests, are invasive and may cause pain, discomfort, and an increased risk of infection. Moreover, they do not support continuous monitoring, which is critical for managing chronic conditions such as diabetes [2]. Consequently, the demand for noninvasive, continuous, and reliable glucose-monitoring techniques is increasing. Researchers are increasingly exploring promising alternatives such as microwave biosensors. The various types of glucose-monitoring techniques are illustrated in Figure 1.

Microwaves (1–300 GHz) are electromagnetic waves that are widely used in healthcare and biosensing. They propagate without a medium, are reflected by metals, and are partially transmitted through nonmetallic materials such as biological tissue, offering both good penetration depth and sensitivity to variations in glucose concentration. Moreover, recent studies have shown that metamaterials can significantly enhance the sensitivity of microwave sensors owing to their engineered electromagnetic properties, which are not observed in natural materials. These structures can concentrate and shape electromagnetic fields, enabling stronger interactions with biomolecules and facilitating noncontact, noninvasive detection, which are key advantages for biomedical applications [3].

Recently, several studies have advanced the field of microwave-based biosensing for noninvasive glucose monitoring. Baghelani et al. developed a chipless printable split-ring resonator (SRR) sensor that enabled real-time glucose detection without complex circuitry, demonstrating the feasibility of low-cost monitoring [4]. Chien designed a 1.8 GHz near-field dielectric plethysmography sensor for heart-rate detection, validating the capability of microwave sensing to monitor physiological changes [5]. Hassan et al. proposed a minimally invasive implantable passive resonator for wireless continuous glucose monitoring, offering reliable operation with reduced discomfort [6]. Omer et al. used whispering gallery mode resonators at millimeter-wave frequencies to characterize aqueous glucose solutions, achieving high sensitivity with the strong confinement of the electromagnetic field [7].

Souza et al. employed double-circular SRRs to evaluate artificial blood plasma solutions, and achieved good sensitivity and reproducibility [8]. Omer et al. proposed a hexagonal complementary SRR (CSRR) sensor on an FR4 substrate that operates near 2.45 GHz and validated it through both Vector Network Analyzer (VNA) measurements and in vivo fingertip tests [9]. In vitro tests of this sensor over the 40–500 mg · dL^{-1} range demonstrated a sensitivity of 0.94 MHz/mg · dL^{-1}. Harnsoongnoen et al. reported a planar microwave sensor fabricated on Rogers

RT/duroid 6002 for fingertip glucose detection with a nonlinear signal response, demonstrating a sensitivity of 0.282 dB/(mg · dL^{-1}) [10]. Hosseinzadeh and Pakvarjouy developed a single-port microwave sensor integrating interdigital and CSRR structures on FR4 that detected glucose in distilled water and saline solutions with limits of detection of 3 and 5 mM, respectively [11]. Srisai et al. [12] demonstrated a noncontact microwave sensor coupled with an artificial neural network for enhanced prediction accuracy, whereas Marzouk et al. [13] introduced a rectangular dielectric resonator system capable of comprehensive, noninvasive glucose monitoring. Other studies have similarly demonstrated high sensitivity to subtle changes in glucose levels using metamaterial-based microwave sensors.

However, limited studies have optimized sensor geometry specifically focusing on fingertip compatibility. Despite prior work employing various microwave and metamaterial geometries, further improvement is needed in two key areas: (i) optimizing the electric field (EF) distribution to enhance sensitivity and (ii) matching the physical dimensions of the sensor to the fingertip anatomy for better electromagnetic coupling. Moreover, reducing the fabrication complexity, such as implementing the sensor in a single-metallic-layer design, can support manufacturability and integration into practical systems [14]. To address these limitations, this study proposes a metamaterial-based microwave sensor that offers several advantages, including a compact design, low sample requirements, and a fingertip-compatible geometry. The integration of this sensor into wearable or noninvasive glucose-monitoring platforms will provide significant advantages in terms of portability, real-time monitoring, and user convenience.

2. METHODOLOGY

2.1. Sensor Design and Optimization. The primary design objective of this study was to develop a compact sensor structure with dimensions compatible with fingertip-scale applications, enabling its potential use in noninvasive glucose detection systems. The proposed microwave metamaterial glucose sensor was designed and evaluated using the CST Microwave Studio simulation software to numerically analyze its electromagnetic response and EF distribution within the sensing region. The sensor structure, shown in Figure 2 (a), comprises a coplanar waveguide (CPW) integrated with symmetrically arranged nested square SRRs. The CPW configuration enables the resonators to be implemented within a single metallic layer, simplifying the fabrication compared to that of the multilayer structures reported in the literature. Design adjustments were performed iteratively, and the geometry was modified and evaluated in the simulation until satisfactory resonance characteristics and strong field localization in the sensing region were achieved.

The substrate material plays a critical role in the electromagnetic performance of microwave sensors. An appropriate substrate should ensure low dielectric loss, a moderate dielectric constant, and good mechanical stability. FR4 was selected as the substrate for this study owing to its affordability, availability, and acceptable microwave performance. The thickness and dielectric constant (ε_r) of the substrate were 1.56 mm and ~4.7, respectively. The conductive layer comprised a 35 μm thick copper film.

2.1.1. Geometrical design. The overall sensor dimensions were 31.51 mm in width and 29.25 mm in height. The side length,

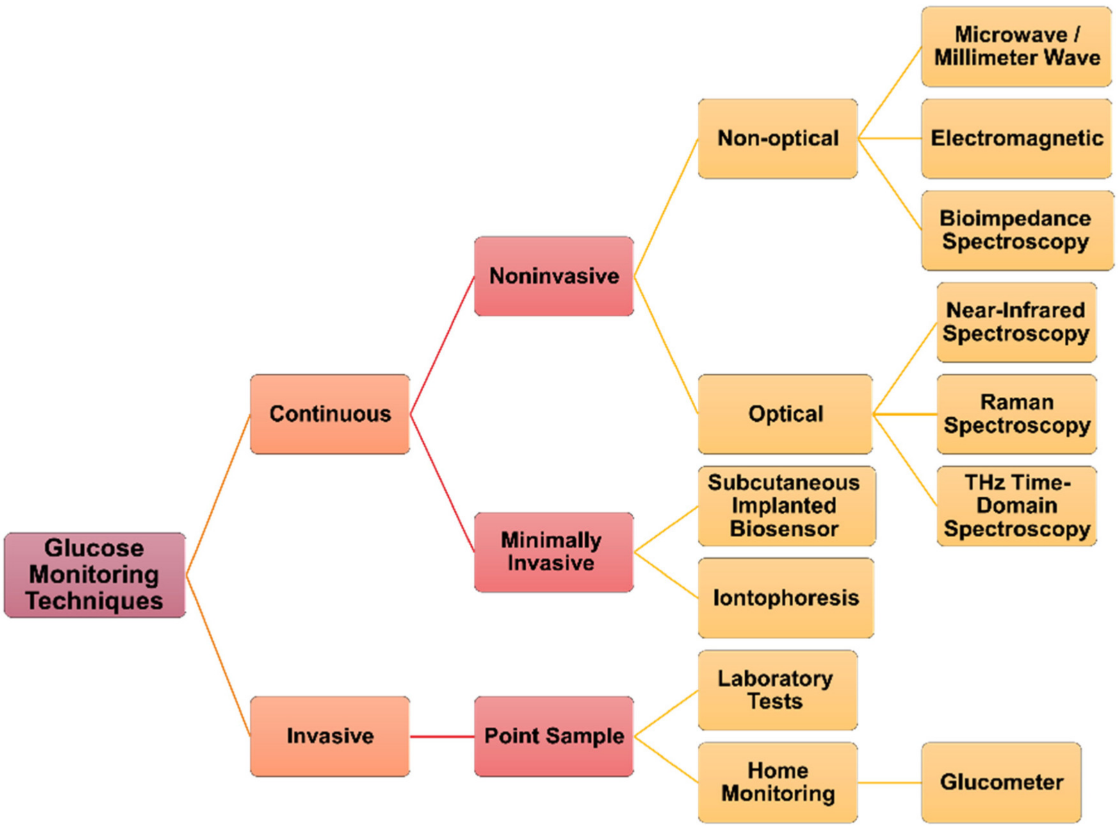

Figure 1. Different techniques for blood glucose monitoring

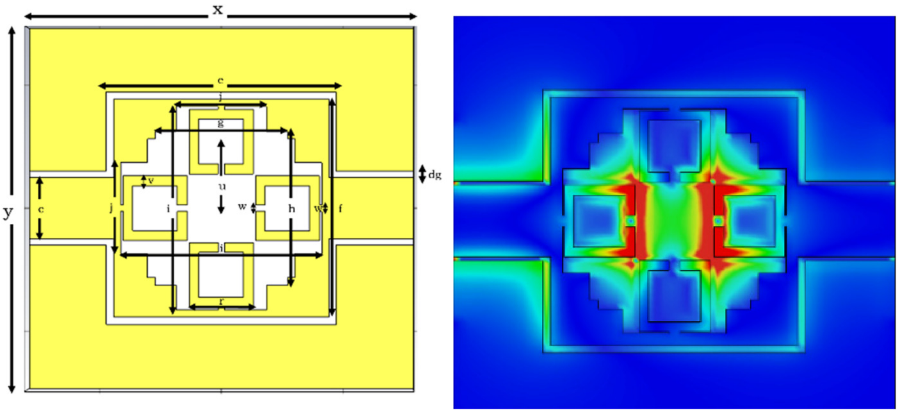

(a) (b)

Figure 2. (a) Geometry of proposed metamaterial microwave glucose sensor indicating the key parameters on an FR4 substrate; (b) Electric field distribution of the sensor at the resonance frequency, showing strong field localization

conductor width, and resonator gaps of each SRR were 5.25, 0.4, and 0.77 mm, respectively. The horizontal and vertical lengths of the resonator frame were 18.88 and 17.68 mm, respectively. The main dimensions of the sensor were selected to match the size of a human fingertip, whereas the other parameters were optimized to achieve a deep and sharp transmission response. The geometry was iteratively refined in the simulation software by modifying the resonator and CPW dimensions until the desired resonance behavior and field localization were obtained.

To ensure appropriate impedance matching, the CPW dimensions were adjusted to obtain a characteristic impedance of approximately 50 Ω. When the gap between the ground planes was 0.5 mm and the signal line width was 5 mm, the resulting impedance closely matched the standard 50 Ω, thereby minimizing the signal reflection and enabling efficient power transfer when connected to a VNA. As shown in Figure 2 (b), the symmetrical SRR arrangement produced a strongly localized EF at the center of the structure, where the sensing sample, such as a glucose solution or fingertip, interacts with the resonant field. This confined EF region significantly enhanced the sensitivity of the sensor to changes in the dielectric properties due to varying glucose concentrations.

The sensor was simulated using the time-domain solver of the CST Microwave Studio Suite. Waveguide ports were placed at both ends of the CPW feed to excite the structure and extract the scattering (S)-parameters (S_{11} and S_{21}) over a frequency range of 2–6 GHz. The simulated response exhibited a resonant frequency of approximately 4.27 GHz.

3. EXPERIMENTAL WORK

3.1. Fabrication. After fabrication, the geometrical parameters of the sensor, including the resonator gaps, CPW line width, and substrate thickness, were measured using a calibrated digital caliper with a resolution of 0.1 mm to verify fabrication accuracy. Each dimension was measured multiple times, and the average value was recorded. Minor deviations were observed compared to the design values obtained from the simulation, which can be attributed to the manufacturing tolerances and etching variations associated with the standard printed circuit board fabrication. For example, the FR4 substrate thickness increased from the intended value of 1.56 mm to approximately 1.7 mm, whereas the inner gap of the resonators increased from 0.77 mm to approximately 0.8 mm. These deviations were within acceptable fabrication limits and did not significantly affect the electromagnetic response of the sensor.

Figure 3 illustrates the fabricated sensor and highlights the observed dimensional variations. The fabricated sensor exhibited a measurable shift in the resonant frequency relative to the simulation results, as listed in Table 1. In the CST Microwave Studio simulations, the design featured a resonance at 4.27 GHz; however, during the VNA measurements, the resonance frequency was 4.18 GHz, exhibiting a discrepancy of only 0.09 GHz. This

Table 1. *Comparison Between Designed and Fabricated Parameters*

Parameter	Simulation	Fabricated	Parameter	Simulation	Fabricated
Width (x)	31.51	31.6	h	12.44	12.5
Length (y)	29.25	29.3	i	16.48	16.2
Thickness (z)	1.56	1.7	j	7.44	7.45
Signal line width is 5 (c)	5	5.1	SRR side length (r)	5.25	5.1
Resonator frame horizontal length (e)	18.88	18.85	Conductor width (v)	0.4	0.7
Resonator frame vertical length (f)	17.68	17.8	Resonator gaps (w)	0.77	0.8
g	10.89	10.2	CPW line width (dg)	0.3	0.3

shift may have resulted from dimensional deviations during fabrication or tolerances in the dielectric constant (ε_r) of the FR4 substrate. Despite this variation, the measured resonance closely aligned with the simulated result, confirming the validity of the sensor design.

3.2. Test Setup. All measurements were performed using a Keysight N9914B VNA. Before data collection, a calibration procedure was conducted to eliminate the effects of cable loss and connector imperfections, as illustrated in Figure 3 (a). Following calibration, the VNA was used to record the reflection (S_{11}) and transmission (S_{21}) coefficients under various test conditions, including distilled water and glucose solutions. Figure 3 (b) shows a comparison of the simulated S_{21} response with its measured counterpart.

3.3. Experimental Samples. Glucose solutions with concentrations of 100, 200, 300, and 400 mg/dL were prepared in distilled water using the mass–volume method. Glucose powder was weighed using a calibrated analytical balance, dissolved in distilled water, and transferred to volumetric containers to ensure accurate dilution. To ensure homogeneity, the solutions were stirred continuously until complete dissolution was achieved. The concentration of each solution was calculated using the following formula.

$$C\left(\frac{mg}{dL}\right) = \frac{\text{mass of glucose (mg)}}{\text{volume of solution (dL)}}$$

A fixed volume of 150 µL was dispensed using a calibrated micropipette into a 3D-printed sensing cell (10 mm ×10 mm ×2

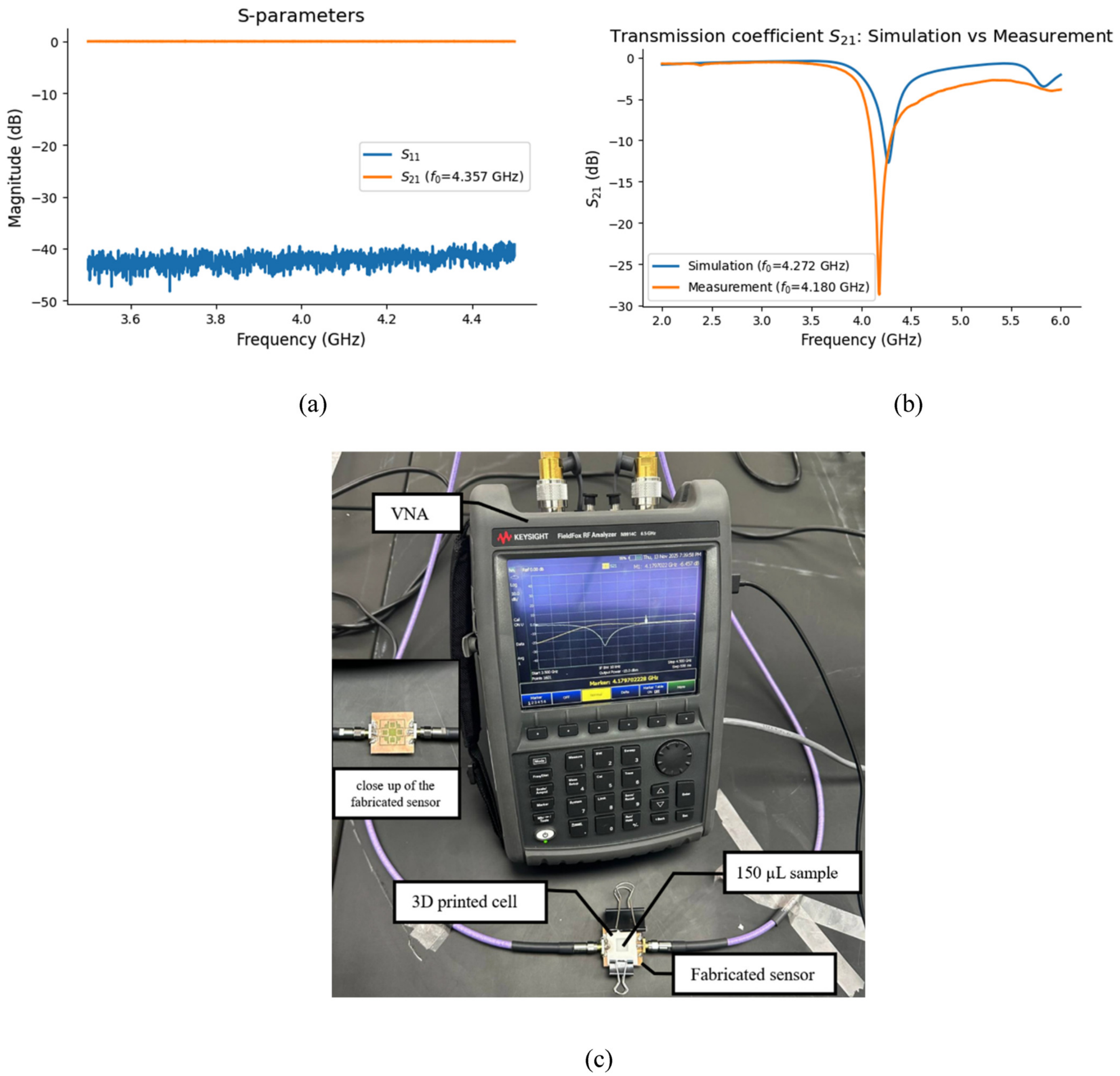

Figure 3. (a) S-parameters after performing the calibration; (b) Simulated and measured S_{21} values across the 2–6 GHz frequency range; (c) Experimental setup with the resonator and 3D printed cell

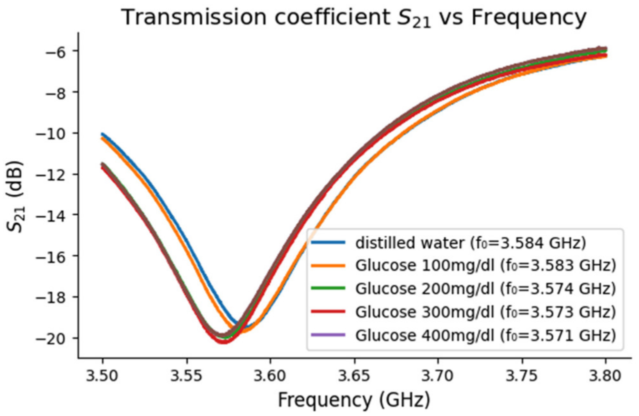

Figure 4. Measured S_{21} response of the fabricated sensor for distilled water and glucose solutions (100–400 mg/dL)

mm) fabricated from polylactic acid-based material, as shown in Figure 3 (c). Each sample was carefully placed over the sensing region to maintain consistent electromagnetic interaction. All measurements were conducted at room temperature (approximately 25 °C).

3.4. Experimental Measurements. For each prepared glucose concentration, the sensor was connected to a calibrated VNA, and S_{21} was measured across the operating frequency range. The resonant frequency for each sample was determined by identifying the minimum magnitude of the S_{21} response. A reference measurement was obtained using distilled water, and the frequency shifts for all glucose concentrations were calculated relative to this baseline. The data-collection process involved detecting the resonance dip and extracting the corresponding resonant frequency for each sample. These values were compiled to evaluate the sensor response to various glucose concentrations.

All data processing steps, including resonance dip identification, frequency extraction, visualization, and regression analysis, were performed using Python to ensure reproducibility and automation. A calibration curve was constructed by plotting the extracted resonant frequencies against the corresponding glucose concentrations. Linear regression was applied to model the relationship between glucose level and frequency shift, with the slope of the resulting line representing the sensitivity of the sensor, which is expressed in $\text{kHz}/(\text{mg} \cdot \text{dL}^{-1})$.

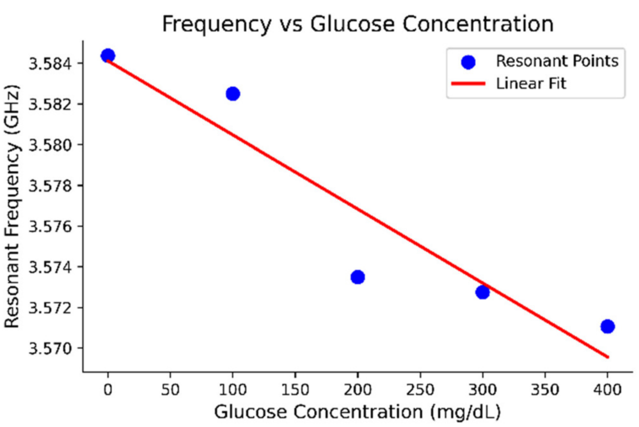

Figure 5. Calibration curve showing resonant frequency as a function of glucose concentration with fitting

4. RESULTS AND DISCUSSION

4.1. S_{21} Frequency Response for Glucose Concentrations. Figure 4 shows the measured S_{21} response of the fabricated sensor for distilled water and glucose solutions with concentrations ranging from 100 to 400 mg/dL. A distinct resonance dip was observed in all measurements, accompanied by amplitude variations. As the glucose concentration increased, the resonance curve progressively shifted toward lower frequencies. Distilled water exhibited the highest resonant frequency at 3.584 GHz, whereas the lowest value (~3.571 GHz) was recorded for the 400 mg/dL sample. This trend indicates that increasing the glucose concentration modified the dielectric properties of the test sample, which directly influenced the electromagnetic response of the sensor.

4.2. Sensitivity. The calibration curve illustrated in Figure 5 shows a clear inverse relationship between the glucose concentration and resonant frequency. Linear regression analysis revealed a sensitivity of approximately 36.4 $\text{kHz}/(\text{mg} \cdot \text{dL}^{-1})$, indicating that for every 1 mg/dL increase in glucose concentration, the sensor exhibits a frequency shift of approximately 36.4 kHz. Although this sensitivity is moderate, the value is highly promising given the simplicity of the sensor and minimal sample volume requirement. Deviations from ideal linearity may result from experimental limitations such as marginal temperature variations, inhomogeneous sample distribution, or mechanical disturbances. Future improvements could involve the implementation of a temperature-controlled measurement setup and a microfluidic channel to stabilize the sample and improve repeatability.

A comparative overview of recent microwave glucose sensors is presented in Table 2. Notably, previous designs predominantly required large sample volumes (up to 3000 µL), limiting their practicality for point-of-care use. Conversely, the proposed sensor achieves a full clinical glucose concentration range (0–400 mg/dL) using only 150 µL of solution. Operating at 4.18 GHz, it balances compact form factor, fabrication simplicity, and low-volume usage. These advantages make the proposed sensor a compelling candidate for integration into wearable or noninvasive glucose-monitoring platforms. In the future, the sensor can be fabricated on lower-loss substrates with significantly smaller loss tangents. Moreover, the sample cell can be manufactured from materials with a lower dielectric loss than that of polylactic acid. These enhancements should reduce the dissipative losses and improve the sensor sensitivity.

Although the sensitivity of the proposed sensor is moderate compared to that of certain high-performance designs, important tradeoffs must be considered, including sample volume, structural simplicity, and fabrication practicality. Compact design, low sample requirements, and fingertip-compatible geometry provide significant advantages for noninvasive sensing applications, where user comfort and integration into portable systems are essential. Overall, the sensor demonstrates a well-balanced solution, and future optimization efforts may further enhance its sensitivity.

Table 2. *Comparison Table*

Reference	Sample type	Sample volume (μL)	Concentration range (mg/dL)	Material	Dimension (mm ^{2})	Operating frequency (GHz)	Sensing parameter	Advantages	Drawbacks
[9]	Aqueous glucose	600	70,90,110,1000	FR4	66 ×1.5	2.45	S_{21}	-High sensitivity -Compact and low cost -Enhanced field interaction -Application of machine learning	-Large sample volume -High loss tangent
[10]	Aqueous glucose	200	0-200	Rogers RO6002	60 ×26	1-1.6	S_{11}	-Use of tube chamber -Integration of machine learning	-Sensitivity variation -Nonlinear response
[12]	Aqueous glucose	3000	0-200	DiClad 880	706.5 (sensor area, based on 30 mm diameter)	2-3	S_{Fr}	-Compact single-port design -Simple setup -Good sensitivity	-Large sample volume -Sensitivity variation -Limited to liquid samples
[15]	Finger phantoms	-	0-500	FR4	35 ×13.5	2.45	S_{11}	-Use of a solid phantom model -Good sensitivity -Compact size	-Sensitivity variation -Nonlinear response
This work	Aqueous glucose	150	0-400	FR4	31.51×29.25	4.18	S_{21}	-Compact, simple fabrication -Smallest sample volume	-High loss tangent

5. CONCLUSIONS

This study investigated a compact metamaterial-based microwave sensor designed for potential noninvasive glucose detection using a fingertip-compatible geometry. The sensor comprised SRRs integrated into a single metallic layer of a CPW structure, demonstrating a simple fabrication as compared to the complex processes associated with the double-layer printed circuit boards that are commonly reported in the literature. The resonance characteristics and sensitivity of the sensor to varying glucose concentrations were evaluated through numerical simulations and experimental validation. The fabricated sensor exhibited a measurable resonance shift with increasing glucose concentration, confirming its ability to detect dielectric variations in aqueous glucose solutions. The calibration curve demonstrated a negative linear relationship between glucose concentration and resonant frequency, with a measured sensitivity of approximately 36.4 $\mathrm{kHz}/(\mathrm{mg}\cdot\mathrm{dL}^{-1})$. Factors such as temperature variation, sample homogeneity, and fabrication tolerance may influence performance. Nevertheless, these results support the feasibility of using metamaterial resonators for glucose monitoring. Overall, the findings highlight the potential of the proposed sensor as a foundation for future noninvasive real-time glucose measurement systems. Future work may include temperature-controlled testing, improved sample handling, integration with portable wireless electronics, and evaluation of human samples to advance practical applications.

AFFILIATIONS AND AUTHOR DETAILS

Undergraduate Author

Dhay Al-Harthi – *Department of Bioengineering, King Fahd University of Petroleum & Minerals, Dhahran 31261, Saudi Arabia*; 0009-0001-6270-1561
Email: s202251020@kfupm.edu.sa

Corresponding Author

Ibraheem Al-Naib – *Research Mentor, Professor, Department of Bioengineering and Center for Biosystems and Machines, King Fahd University of Petroleum & Minerals, Dhahran 31261, Saudi Arabia*; 0000-0002-7499-0655
Email: ibraheem.naib@kfupm.edu.sa

ACKNOWLEDGEMENTS

The authors acknowledge the support provided by the Department of Bioengineering at King Fahd University of Petroleum and Minerals. The authors also extend their appreciation to the technical staff and laboratory team for their assistance with specimen preparation and testing.

REFERENCES

(1) World Health Organization. Global report on diabetes. WHO Press (2022).

(2) American Diabetes Association. Standards of medical care in diabetes—2023. *Diabetes Care* **46**, S1–S291 (2023).

(3) Teymoori, M. & Yalçınkaya, A. D. A low-cost microwave metamaterial-inspired sensing platform for quantitative paper microfluidic analytical devices. *Sens. Actuators A Phys.* **363**, 114684 (2023).

(4) Baghelani, M., Abbasi, Z., Daneshmand, M. et al. Non-invasive continuous-time glucose monitoring system using a chipless printable sensor based on split ring microwave resonators. *Sci. Rep.* **10**, 12980 (2020).

(5) Chien, J.-C. A 1.8-GHz near-field dielectric plethysmography heart-rate sensor with time-based edge sampling. *IEEE J. Solid-State Circuits* **55**, 615–628 (2020).

(6) Hassan, R. S., Lee, J. & Kim, S. A minimally invasive implantable sensor for continuous wireless glucose monitoring based on a passive resonator. *IEEE Antennas Wireless Propag. Lett.* **19**, 124–128 (2020).

(7) Omer, A. E., Gigoyan, S., Shaker, G. & Safavi-Naeini, S. WGM-based sensing of characterized glucose–aqueous solutions at mm-waves. *IEEE Access* **8**, 38809–38825 (2020).

(8) Souza, M. I. O., Santos, N. M., Alarcon, J. C. P., Varanda, L. C., Pepino, V. M. & Borges, B.-H. V. Microwave glucose sensing using double circular split ring resonators for improved sensitivity: the role of artificial blood plasma and deionized water. *IEEE Sens. J.* **25**, 4529–4540 (2025).

(9) Omer, A. E., Shaker, G., Safavi-Naeini, S. et al. Low-cost portable microwave sensor for non-invasive monitoring of blood glucose level: novel design utilizing a four-cell CSRR hexagonal configuration. *Sci. Rep.* **10**, 15200 (2020).

(10) Harnsoongnoen, S., Srisai, S., Kongkeaw, P. & Buranrat, B. Detection and classification of glucose solution concentration and blood sugar levels at the fingertip using a novel planar microwave sensor and deep learning techniques. *Sens. Actuators B Chem.* **430**, 137322 (2025).

(11) Hosseinzadeh, S. & Pakvarjouy, M. Microwave-based single port glucose sensor arranging interdigital and complementary split ring resonator. *Measurement* **246**, 116695 (2025).

(12) Srisai, S., Kongkeaw, P. & Harnsoongnoen, S. Noncontact and noninvasive detection of glucose concentration using a single-port microwave sensor coupled with artificial neural networks. *IEEE Trans. Instrum. Meas.* **74**, 1–10 (2025).

(13) Marzouk, H. M., Abd El-Hameed, A. S., Allam, A., Pokharel, R. K. & Abdel-Rahman, A. B. Comprehensive system for noninvasive glucose monitoring utilizing a rectangular dielectric resonator microwave sensor. *IEEE Trans. Instrum. Meas.* **74**, 4003413 (2025).

(14) Martins, A. J. L., Velásquez, R. J., Gaillac, D. B., Santos, V. N., Tami, D. C., Souza, R. N. P., Osorio, F. C., Fogli, G. A., Soares, B. S., Rego, C. G. D., Medeiros-Ribeiro, G., Drummond, J. B., Mosquera-Lopez, C. M. & Ramirez, J. C. A comprehensive review of non-invasive optical and microwave biosensors for glucose monitoring. *Biosens. Bioelectron.* **271**, 117081 (2025).

(15) Jeong, J.-M., Bien, F. & Lee, J.-G. Design of orientation-independent non-invasive glucose sensor based on meta-structured antenna. *Electronics* **14**, 2295 (2025).